Pure and Applied Mathematics Journal
2022; 11(6): 102-111
http://www.sciencepublishinggroup.com/j/pamj
doi: 10.11648/j.pamj.20221106.12
ISSN: 2326-9790 (Print); ISSN: 2326-9812 (Online)

Unique Diagram of a Spatial Arc and the Knotting Probability

Akio Kawauchi

Osaka Central Advanced Mathematical Institute, Osaka Metropolitan University, Osaka, Japan

Email address:
kawauchi@omu.ac.jp

To cite this article:
Akio Kawauchi. Unique Diagram of a Spatial Arc and the Knotting Probability. *Pure and Applied Mathematics Journal*. Vol. 11, No. 6, 2022, pp. 102-111. doi: 10.11648/j.pamj.20221106.12

Received: November 2, 2022; **Accepted**: November 18, 2022; **Published**: November 29, 2022

Abstract: There is a question of how a spatial polygonal arc in 3-space such as a linear molecule, a protein, a non-circular DNA, or a linear polymer, etc. is considered as a knot object. This paper answers it by introducing a notion of knotting probability of a spatial arc. As a tool, the knotting probability of an arc diagram which is invariant under isomorphisms of arc diagrams has been already established by the author, which measures how many non-trivial ribbon surface-knots of genus 2 in the 4-space occur when the arc diagram is regarded as a ribbon chord diagram in a 4D research object. A main task of this paper is to show how to obtain an arc diagram uniquely up to isomorphisms from a given oriented spatial polygonal arc. The image of an oriented spatial polygonal arc under the orthogonal projection from the 3-space to a plane along a unit normal vector is not always any arc diagram. It is shown that an arc diagram unique up to isomorphisms which is determined only by the unit normal vector can be obtained by approximating the projection image of an oriented spatial polygonal arc. By combining the resulting arc diagram with the knotting probability of an arc diagram already established, the knotting probability of every spatial polygonal arc belonging to a unit vector is defined. It is also observed that every oriented spatial polygonal arc (except for the case of a polygonal arc contained in a straight line segment) in 3-space admits a unique orthonormal basis of the 3-space. Thus, the knotting probability of a spatial polygonal arc in 3-space is defined. The knotting probabilities of three concrete examples on oriented spatial polygonal arcs are computed.

Keywords: Arc Diagram, Approximation, Spatial Arc, Knotting Probability

1. Introduction

A *spatial arc* is a polygonal arc (not a straight line segment) embedded in the 3-space R^3, which is considered as a model of a protein or a linear polymer in science. The following question on science is an interesting question that can be set as a mathematical question:

Question. How a linear scientific object such as a linear molecule, a protein, a non-circular DNA, a linear polymer, … is considered as a knot object?

The main purpose of this paper is to show that the projection image of an oriented spatial arc into the oriented plane is approximated uniquely (up to isomorphic arc diagrams) to an arc diagram specified uniquely by the spatial arc and the projection direction. This argument is related to a known argument transforming a classical knot in R^3 into a regular knot diagram. [1, 3] By this argument, the typical 12 arc diagrams determined uniquely (up to isomorphic arc diagrams) by the spatial arc are canonically specified so that the orientation change of the spatial arc makes only a substitution for these arc diagrams. Let

$$S^2=\{ v\in R^3 \mid \|v\|=1\}$$

be the unit sphere, where $\|v\|$ denotes the norm of a vector $v\in R^3$. Every element $u\in S^2$ is regarded as a unit vector from the origin 0. For a unit vector u, let P_u denote the oriented plane containing the origin 0 such that the unit vector u is a positive normal vector to P_u. The orthogonal projection from R^3 to the plane P_u is called the *projection along* the unit vector $u\in S^2$ and denoted by

$$\lambda_u: R^3\to P_u.$$

For a small positive number δ, a δ-*approximation* of the projection $\lambda_u: R^3\to P_u$ along $u\in S^2$ is the projection $\lambda_w: R^3\to P_w$ along a unit vector $w\in S^2$ with $\|w-u\|<\delta$, which is

denoted by

$$\lambda_u^{\delta}: R^3 \to P_u.$$

The projection image $\lambda_u(L)$ of a spatial arc L in P_u is an *arc diagram* in the oriented plane P_u if $\lambda_u(L)$ has only *crossing points* (namely, transversely intersecting double points with over-under information) and further the starting and terminal points as single points. The arc diagram $(P_u, \lambda_u(L))$ is also denoted by (P, D). An arc diagram (P, D) is *isomorphic* to an arc diagram (P', D') if there is an orientation-preserving homeomorphism f: P→P' sending D to D' which preserves the crossing points of D and D', and the starting and terminal points of D and D'. The map f is called an *isomorphism* from D to D'. In an illustration of an arc diagram, it is convenient to illustrate an arc diagram with smooth edges in the class of isomorphic arc diagrams instead of a polygonal arc diagram. In this paper, the following observation is shown.

Theorem 1.1. Let L be an oriented arc in R^3, and $\lambda_u: R^3 \to P_u$ the projection along a unit vector $u \in S^2$. For any sufficiently small positive number δ, the projection λ_u has a δ-approximation

$$\lambda_u^{\delta}: R^3 \to P_u$$

such that the projection image $\lambda_u^{\delta}(L)$ is an arc diagram specified from L and λ_u uniquely up to isomorphic arc diagrams.

The proof of Theorem 1.1 is done in Section 2. By the author's precedent study, the knotting probability

$$p(D) = (p^{I}(D), p^{II}(D), p^{III}(D), p^{IV}(D))$$

of an arc diagram D is defined so that it is unique up to isomorphic arc diagrams. [10] The *knotting probability* p(L; u) of an oriented spatial arc L for every unit vector $u \in S^2$ is defined by

$$p(L;u)=p(D(L;u))$$

for the arc diagram $D(L;u)=\lambda_u^{\delta}(L)$. More details are discussed in Section 3.

We mention here a brief history on researches of knotting probability of a spatial arc. A study of knotting probability on a circular knot has first appeared from the viewpoint of a random knotting different from our viewpoint. [2, 13] Then a study of knotting probability of a spatial arc from a random knotting viewpoint appeared with the same motivation as the present question. [12] Some protein knotting data are listed in "KnotProt" (https://knotprot.cent.uw.edu.pl/). Another study of knotting probability on a spatial arc appeared by using a knotting structure of a spatial graph but with the demerit that it depends on the heights of the crossing points of a diagram of the spatial arc. [4, 6]

In Section 2, the proof of Theorem 1.1 is done. In Section 3, the knotting probability of a spatial arc with a given direction of the projection is explained. In Section 4, the knotting probabilities of some spatial arcs are computed.

2. Proof of Theorem 1.1

Let L be an oriented spatial arc with the starting point s and the terminal point t. Let $u(\beta) \in S^2$ be the unit vector of an oriented (straight) line β in R^3. The *front edge* of L is the line segment γ in R^3 joining the starting point s and the terminal point t. Orient γ by the orientation from s to t. The *front line* β(γ) is the oriented line extending the oriented front edge γ of L. The unit vector u(γ) of β(γ) is called the *front edge vector* of L. An *edge line* of L is an oriented line in R^3 extending an oriented edge of L. The *starting front-pop line* of L is the edge line β(s) of the edge which pops for the first time from the front line β(γ) when a point is going on the oriented spatial arc L. The *ending front-pop lin*e of L is the edge line β(t) of the edge which reaches the front line β(γ) at the end when a point is going on the oriented spatial arc L. The unit vectors of β(s) and β(t) are called the *starting* and *terminal front-pop vectors* and denoted by u(s) and u(t), respectively. The *starting front-pop plane* of L is the oriented plane P(γ,s) determined by the front line β(γ) and the starting pop line β(s) in this order. The *terminal front-pop plane* of L is the oriented plane P(γ,t) determined by the front line β(γ) and the terminal pop line β(t) in this order. For a plane P in R^3, the *great circle* C of P is the great circle in S^2 obtained as the intersection of S^2 and the plane P' with the origin 0 which is parallel to P.

Definition. The *trace set* T of L is the subset of S^2 consisting of the unit vectors and the great circles obtained from L in the following cases (i) and (ii).

(i). The great circle C of the plane determined by an edge line β and a vertex v of L disjoint from β or the plane determined the front line β(γ) and a vertex v of L disjoint from β(γ).

(ii). The unit vectors $\pm u(\eta) \in S2$ of an oriented line η in R3 intersecting three lines consisting of three distinct edge lines βi (i = 1, 2, 3) or two distinct edge lines βi (i=1, 2) and the front line β(γ) of L any two lines of which are not on the same plane.

It is known that the set X consisting of the unit vectors $\pm u(\eta) \in S^2$ in (ii) is a piecewise smooth graph in S^2 invariant under the antipodal involution -1 of S^2 sending (x, y, z) to (-x,-y,-z). [1, 3, 14] In fact, X is considered as the union $Y \cup -1(Y)$ for a conic section Y of a quadratic surface in R^3. Thus, the trace set T is a piecewise smooth graph in S^2 which is invariant under the antipodal involution -1. The following lemma is shown.

Lemma 2.1. For every unit vector $u \in S^2$-T, the projection image $\lambda_u(L)$ is an arc diagram in the plane P_u which is independent of a choice of unit vector u in a connected component R of S^2-T up to isomorphisms.

Proof of Lemma 2.1. The unit vectors $\pm u(\eta) \in S^2$ of a line η joining two distinct vertexes of L are in T by (i). Let a unit vector $u \in S^2$ be not in (i). Then the set of vertexes of L is embedded in P_u by λ_u. Every edge line and the front line β(γ) of L are embedded in the plane P_u by the projection λ_u so that any two distinct parallel lines on them are disjointedly embedded in P_u (since λ_u is a linear map). Further, the image of the set of vertexes of L is disjoint from the images of the

interiors of all the edges of L and the front edge γ. If a unit vector $u \in S^2$ is in neither (i) nor (ii), then the images of the edges of L intersect only among the images of the interiors of the edges of L. Every intersection point is a double point, since a line η in R^3 intersecting three distinct lines in the edge lines and the front line $\beta(\gamma)$ of L is in the trace set T. Thus, the projection image $\lambda_u(L)$ is an arc diagram in the plane P_u. Let R be a connected component of S^2-T. The arc diagram $\lambda_u(L)$ is the same arc diagram up to isomorphisms for all unit vectors u in a connected open neighborhood in R and thus for all unit vectors u in R. This completes the proof of Lemma 2.1.

The proof of Theorem 1.1 is done as follows:

Proof of Theorem 1.1. The idea of the proof is to specify, for any given unit vector $u \in S^2$, a unique connected component R of S^2-T such that R intersects any small open neighborhood of u in R^3. If $u \in S^2$-T, then take the connected component R containing u. Assume that $u \in T$. To do this specification, for any given oriented spatial arc L, the new x-axis, y-axis and z-axis of the 3-space R^3 are set as follows:

The front edge vector $u(\gamma)$ of the front edge γ is taken as the unit vector of the x-axis:

$$u(\gamma)=u_x=(1, 0, 0).$$

Let $u_y \in S^2$ be the unit vector orthogonal to the front edge vector $u_x=u(\gamma)$ in the starting front-pop plane $P(\gamma, s)$ of L with the inner product $(u_y,u(s))$ positive for the starting front-pop vector u(s). The unit vector u_y is taken as the unit vector of the y-axis:

$$u_y=(0, 1, 0).$$

The exterior product $u_z= u_x \times u_y$ gives the z-axis:

$$u_z=(0, 0, 1).$$

Note that the unit vectors u_x, u_y, u_z are uniquely specified by the oriented spatial arc L. Under this setting of the coordinate axis, let S^2 be the unit sphere which is the union of the upper hemisphere $S^2(+)$, the equatorial circle $S^2(0)$ and the lower hemisphere $S^2(-)$ given as follows:

$$S^2(+)=\{(x, y, z) \in R^3 \mid x^2+y^2+z^2=1, z>0\},$$

$$S^2(0)=\{(x, y, z) \in R^3 \mid x^2+y^2+z^2=1, z=0\},$$

$$S^2(-)=\{(x, y, z) \in R^3 \mid x^2+y^2+z^2 =1, z<0\}.$$

The equatorial circle $S^2(0)$ belongs to T since the starting front-pop plane $P(\gamma, s)$ of L coincides with the plane with z=0. Every unit vector $u \in S^2(+) \cup S^2(0)$ except for the north pole (0, 0, 1) is uniquely written as

$$u=\varphi(r, \theta)=(r \cos \theta, r \sin \theta, \sqrt{1-r^2})$$

for real numbers r and θ with $0<r \leqq 1$ and $0 \leqq \theta<2\pi$ in a unique way.

Case 1: $u=\varphi(r,\theta) \in S^2(+)-\{(0,0,1)\}$.

Consider the half-open arc

$$\varphi_r[\theta,\theta+\varepsilon)=\{\varphi(r, \theta_+)| \ \theta \leqq \theta_+<\theta+\varepsilon\}$$

for a sufficiently small positive number ε. If $\varphi_r[\theta,\theta+\varepsilon)$ meets T only with u, then specify as R the connected component of $S^2(+)$-T containing the open arc $\varphi_r[\theta,\theta+\varepsilon)-\{u\}$. If the half-open arc $\varphi_r[\theta,\theta+\varepsilon)$ is in T for a sufficiently small positive number ε, then consider a sufficiently small disk d in S^2 with the center u so that the intersection $I_1=\varphi_r[\theta,\theta+\varepsilon) \cap d$ is a line segment in $\varphi_r[\theta,\theta+\varepsilon)$ and the intersection $T \cap d$ is the union of simple arcs I_i (i= 1, 2,..., m) in d meeting only at u and joining u with boundary points b_i (i= 1, 2,..., m) of d. Since the disk d is canonically oriented, assume that the points b_i (i= 1, 2,..., m) are enumerated along the orientation of the boundary circle of d. Then specify as R the connected component of $S^2(+)$-T containing the interior of the region in d bounded by I_1 and I_2 among the regions in d divided by I_i (i= 1, 2,..., m).

Case 2: $u=(0,0,1) \in S^2(+)$.

The half-open arc

$$\varphi^0[0,r) = \{\varphi(r_-, 0)| \ 0 \leqq r_-<r\}$$

is considered for a sufficiently small positive number r. If the half-open arc $\varphi^0[0,r)$ meets T only with u, then specify as R the connected component of $S^2(+)$-T containing the open arc $\varphi^0[0,r)-\{u\}$.

If the half-open arc $\varphi^0[0,r)$ is in T for a sufficiently small positive number r, then a sufficiently small disk d in S^2 with the center u is considered so that the intersection $I_1=\varphi^0[0,r) \cap d$ is a line segment in $\varphi_0[0,r)$ and the intersection $T \cap d$ is the union of simple arcs I_i (i= 1, 2,..., m) in d meeting only at u and joining u with boundary points b_i (i= 1, 2,..., m) of d. Since the disk d is canonically oriented, assume that the points b_i (i= 1, 2,..., m) are enumerated along the orientation of the boundary circle of d. Then specify as R the connected component of $S^2(+)$-T containing the interior of the region in d bounded by I_1 and I_2 among the regions in d divided by I_i (i= 1, 2,..., m).

Case 3: $u=\varphi(1,\theta) \in S^2(0)$.

Let $0 \leqq \theta<\pi$. Consider the half-open arc

$$\varphi_1[\theta,\theta+\varepsilon)=\{\varphi(1,\theta_+)| \ \theta \leqq \theta_+<\theta+\varepsilon\}$$

for a sufficiently small positive number ε with $\theta+\varepsilon<\pi$. Since the half-open arc $\varphi_1[\theta,\theta+\varepsilon)$ is in T, consider a sufficiently small disk d in S^2 with the center u so that the intersection $I_1=\varphi_1[\theta,\theta+\varepsilon) \cap d$ is a line segment in $\varphi_1[\theta,\theta+\varepsilon)$ and the intersection $T \cap d$ is the union of simple arcs I_i (i= 1, 2,..., m) in d meeting only at u and joining u with boundary points b_i (i= 1, 2,..., m) of d. Since the disk d is canonically oriented, assume that the points b_i (i= 1, 2,..., m) are enumerated along the orientation of the boundary circle of d. Then specify as R the connected component of $S^2(+)$-T containing the interior of the region in d bounded by I_1 and I_2 among the regions in d divided by I_i (i= 1, 2,..., m). Let $\pi \leqq \theta<2\pi$. Since the antipodal vector-$u=\varphi(1,\theta-\pi)$ of u is in $S^2(0)$ with $0 \leqq \theta-\pi<\pi$,

let R(-) be the connected component of S^2-T specified for-u. As the connected component R of S^2-T for u, specify the image of R(-) under the antipodal involution -1 of S^2.

Case 4: $u \in S^2(-)$.

Since the antipodal unit vector -u of u is in $S^2(+)$, let R(-) be the connected component of S^2-T specified for -u in Cases 1 and 2. As the connected component R of S^2-T for u, specify the image of R(-) under the antipodal map -1 of S^2.

Thus, for every unit vector $u \in S^2$, the connected component R of S^2-T is uniquely specified. By Lemma 2.1, for every unit vector $u \in R$, the image $\lambda_u(L)$ of L under the projection λ_u: $R^3 \to P_u$ along u is an arc diagram determined from L and λ_u uniquely up to isomorphisms. Since any open neighborhood of the unit vector u in R^3 intersects the specified connected component R, for every $u \in S^2$ and every $\delta>0$, there is a unit vector w in the specified component R for u such that $\|w-u\|<\delta$ and the projection λ_w: $R^3 \to P_w$ along w is a desired δ-approximation λ_u^{δ}: $R^3 \to P_u$ of the projection λ_u: $R^3 \to P_u$ along u. This completes the proof of Theorem 1.1.

The orthogonal projection λ_u: $R^3 \to P_u$ for the unit vector $u = u_x$, u_y or u_z in the proof of Theorem 1.1 is denoted by

$$\lambda_x: R^3 \to P_x,\ \lambda_y: R^3 \to P_y \text{ or } \lambda_z: R^3 \to P_z,$$

and the arc diagram $D(L;u)=\lambda_u^{\delta}(L)$ is denoted by D(L;x), D(L;y) or D(L;z), respectively. The arc diagram D(L;-u) is also denoted by D(L;-x), D(L;-y) or D(L;-z), respectively. An arc diagram D in a plane P is *inbound* if the starting point s and the terminal point t of the arc diagram D are in the same region of the plane P divided by the arc diagram D. More generally, the projection image $\lambda_u(L)$ of a spatial arc L which need not be an arc diagram is *inbound* if the projection images $\lambda_u(L-\partial\gamma)$ and $\lambda_u(\gamma)$ are disjoint for the front edge γ of L. A spatial arc L is an *arc knot* if the union cl(L) of L and the front edge γ of L is a knot (i.e., a simple closed curve) in R^3. The knot cl(L) is called the *closed knot* of L. A spatial arc L is *even* if the starting front-pop plane $P(\gamma, s)$ and the terminal front-pop plane $P(\gamma, t)$ are the same. Let -L denote the same spatial arc as L but with the opposite orientation. The following observations are obtained from the proof of Theorem 1.1.

Corollary 2.2. For the arc diagram $D(L;u) = \lambda_u^{\delta}(L)$ of an oriented spatial arc L for a unit vector $u \in S^2$, the following properties (1)-(5) are obtained.

(1) The arc diagram D(L;-u) is the mirror image of D(L;u) meaning that the upper-lower relations of the crossing points of D(L;u) and D(L;-u) are exchanged all at once.
(2) If the projection image $\lambda_u(L)$ is an arc diagram, then the arc diagram D(L;u) is equal to $\lambda_u(L)$ up to isomorphisms of arc diagrams.
(3) There are only finitely many arc diagrams D(L;u) up to isomorphic arc diagrams for all unit vectors $u \in S^2$.
(4) If the projection image $\lambda_u(L)$ is inbound, then the arc diagram D(L;u) is an inbound arc diagram. Thus, if L is an arc knot, then the arc diagram D(L;x) for the front edge vector u_x is an inbound arc diagram.
(5) For an even spatial arc L, the arc diagram D(-L;u) is isomorphic to the arc diagram D(L;u) or the inversed mirror image D(L;-u) of the arc diagram D(L;u) according to whether the orientations of the planes $P(\gamma, s)$ and $P(\gamma, t)$ coincide or not.

3. The Knotting Probability

A *chord graph* is a trivalent connected graph $(o;\alpha)$ in R^3 consisting of a trivial oriented link o (called a *based loop system*) and the attaching arcs α (called a *chord system*), where some chords of α may intersect. A *chord diagram* is a diagram $C(o;\alpha)$ (in a plane) of a chord graph $(o;\alpha)$ in R^3. A *ribbon surface-link* is a surface-link in the 4-space R^4 obtained from a trivial S^2-link by surgery along mutually disjoint embedded 1-handles (see the papers [11, 15] for earlier versions of this concept). A chord diagram C corresponds to a ribbon surface-link F(C) in the 4-space R^4 by a canonical construction so that an equivalence between two ribbon surface-links F(C) and F(C') corresponds to a combination of the moves on a chord diagram called M_0, M_1 and M_2 (see the papers [5, 7, 8, 9] for details). Let D be an oriented n-crossing arc diagram. A chord diagram C with n+2 based loops and n chords is obtained from D by replacing every crossing point and every endpoint with a based loop as in Figure 1.

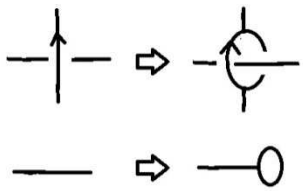

Figure 1. *Transformation of an oriented arc diagram into a chord diagram.*

Let D be an oriented n-crossing arc diagram, and C the chord diagram of D. Let o(s) and o(t) be the based loops in C transformed from the starting and terminal points s and t, respectively. There is a system **A** of $(n+2)^2$ chord diagrams obtained from the chord diagram C by joining the loops o(s) and o(t) with any based loops of C by two chords not passing the other based loops. Every member A of **A** is called an *adjoint chord diagram* of C with an *additional chord pair*. Note that the ribbon surface-knot F(C) of the chord diagram C is a ribbon S^2-knot and the ribbon surface-knot F(A) of an adjoint chord diagram $A \in \mathbf{A}$ is a genus 2 ribbon surface-knot. A chord diagram is said to be *unknotted* or *knotted* according to whether it gives a trivial or non-trivial ribbon surface-knot, respectively. The idea of the knotting probability of the arc diagram D is to measure how many knotted chord diagrams there are in the system **A** of the $(n+2)^2$ adjoint chord diagrams constructed from the chord diagram C of D. Since there are canonical overlaps in **A** up to isomorphisms, the subsystem $\mathbf{A}^*$ of **A** consisting of n^2+2n+2 adjoint chord diagrams of C obtained by removing the canonical overlaps is considered. The subsystem $\mathbf{A}^*$ is classified by the following four types (see the paper [10]):

Type I. Here are the 2 adjoint chord diagrams of C consisting of a chord diagram with two self-attaching chords on o(s) and

o(t) added and a chord diagram with a self-attaching chord on o(s) and a chord joining o(s) with o(t) added.

Type II. Here are the 2n adjoint chord diagrams of C given by additions of n chord pairs consisting of a self-attaching chord on o(s) and a chord joining o(t) with a based loop except for o(s) and o(t), and additions of n chord pairs consisting of a self-attaching chord on o(t) and a chord joining o(s) with a based loop except for o(s) and o(t).

Type III. Here are the n adjoint chord diagrams of C where the additional chord pairs consist of a chord joining o(s) with o(t) and a chord joining o(s) with a based loop except for o(s) and o(t).

Type IV. Here are the n(n-1) adjoint chord diagrams of C where the additional chord pair joins the pair of o(s) and o(t) with a distinct based loop pair not containing o(s) and o(t).

It is shown that every adjoint chord diagram of the chord diagram C of any n crossing arc diagram D is deformed into one of the adjoint chord diagrams of type I, II, III and IV of the chord diagram C. [10] Consequently, it is justified to reduce the $(n+2)^2$ adjoint chord diagrams to the n^2+2n+2 adjoint chord diagrams. The *knotting probability* p(D) of an arc diagram D is defined to be the quadruplet

$$p(D) = (p^I(D), p^{II}(D), p^{III}(D, p^{IV}(D))$$

of the following knotting probabilities $p^I(D)$, $p^{II}(D)$, $p^{III}(D)$, $p^{IV}(D)$ of types I, II, III, IV.

Definition.

(1) Let A_1 and A_2 be the adjoint chord diagrams of type I and assume that there are just k knotted chord diagrams among them. Then the *type I knotting probability* of D is defined to be

$$p^I(D) = \frac{k}{2}.$$

Thus, $p^I(D)$ is 0, 1/2 or 1 for any arc diagram D.

(2) Let A_i(i=1, 2, ... , 2n) be the adjoint chord diagrams of type II and assume that there are just k knotted chord diagrams among them. Then the *type II knotting probability* of D is defined to be

$$p^{II}(D) = \frac{k}{2n}.$$

(3) Let A_i (i=1, 2,...,n) be the adjoint chord diagrams of type III and assume that there are just k knotted chord diagrams among them. Then the *type III knotting probability* of D is defined to be

$$p^{III}(D) = \frac{k}{n}.$$

(4) Let A_i (i=1, 2,...,n(n-1)) be the adjoint chord diagrams of type IV and assume that there are just k knotted chord diagrams among them. Then the *type IV knotting probability* of D is defined to be

$$p^{IV}(D) = \frac{k}{n(n-1)}.$$

The knotting probability p(D) of an arc diagram D is uniquely determined up to isomorphisms of D. If the orientation of an arc diagram D is changed, then all the orientations of the based loops of the chord diagram C are changed at once. This means that the knotting probability p(D) of D does not depend on any choice of orientations of D, and thus, the orientation of D can be omitted in figures. Some calculations of p(D) for an arc diagram D are done so that

$$p^I(D) = 0 \text{ or } 1,\ p^{II}(D) = p^{III}(D) \text{ and } p(D) = p(D^*)$$

for any inbound arc diagram D and the mirror image D^* of D (see the paper [10;Theorem 3.3 (3)] for the proof). The knotting probability p(D) has *p(D)=1* if

$$p^I(D) = p^{II}(D) = p^{III}(D = p^{IV}(D) = 1$$

and otherwise, *p(D) < 1*. The knotting probability p(D) has *p(D)> 0* if

$$p^I(D)+p^{II}(D)+p^{III}(D)+p^{IV}(D) > 0$$

and otherwise, *p(D)=0*. The *knotting probability*

$$p(L;u) = (p^I(L;u), p^{II}(L;u), p^{III}(L;u), p^{IV}(L;u))$$

of an oriented spatial arc L in R^3 along a unit vector $u \in S^2$ is defined to be

$$p(L;u) = p(D(L;u))$$

for the arc diagram $D(L;u)=\lambda_u^{\delta}(L)$ given by Theorem 1.1, which is uniquely determined by the spatial arc L and a unit vector u. For the unit vector $u = u_x$, u_y or u_z, the knotting probabilities $p(L;\pm u)$ are denoted by $p(L;\pm x)$, $p(L;\pm y)$ and $p(L;\pm z)$, respectively. As already observed, the knotting probability p(L;u) is unchanged by any choice of a string orientation in the arc diagram D(L;u). However, because the arc diagram D(L;u) may be much different from the arc diagram D(-L;u) by definition, the knotting probability p(-L;u) of the reversed spatial arc-L (that is the same spatial arc as L but with reversed orientation of L) may be much different from p(L;u) in general. In any case, the unordered pair of p(L;u) and p(-L;u) is considered as the knotting probability of a spatial arc L which is independent of the string orientation. When one-valued probability is needed, a suitable average of the knotting probabilities

$$p^I(\pm L;u),\ p^{II}(\pm L;u),\ p^{III}(\pm L;u),\ p^{IV}(\pm L;u)$$

is considered. The following corollary is obtained for a special case of a spatial arc L.

Corollary 3.1.

(1) If the projection image $\lambda_u(L)$ is inbound, then

$$p(L;u) = p(L;-u),$$

so that if L is an arc knot, then

$$p(L;x) = p(L;-x).$$

(2) If L is even, then

$$p(-L;u) = p(L;u) \text{ or } p(-L;u) = p(L;-u)$$

for any $u \in S^2$ according to whether the orientations of $P(\gamma, s)$ and $P(\gamma, t)$ coincide or not.

(3) If L is even and the projection image $\lambda_u(L)$ is inbound, then the four knotting probabilities

$$p(\pm L;\pm u) \text{ are the same as } p(L;u).$$

Proof of Corollary 3.1. In [10], it is shown that $p(D) = p(D^*)$ for an inbound arc diagram D and the mirror image D^* of D. By Corollary 2.2 (1) and (4), the arc diagrams D(L;u) and D(L;x) are inbound arc diagram with D(L;-u) and D(L;-x) the mirror images. Thus, (1) is obtained. For (2), the arc diagram D(-L;u) is isomorphic to the arc diagram D(L;u) or D(L;-u) according to whether the orientation of $P(\gamma, s)$ coincides with the orientation of $P(\gamma, t)$ or not by Corollary 2.2 (1) and (5). The assertion (3) is a combination result of (1) and (2). This completes the proof of Corollary 3.1.

4. Computing Some Examples

It is stated in Corollary 2.2 (3) that for every spatial arc L, there are only finitely many arc diagrams D(L;u) up to isomorphic arc diagrams for all unit vectors $u \in S^2$. However, it is a very hard problem to enumerate all the arc diagrams D(L;u) even for a simple spatial arc L. By this reason, some specific arc diagrams that can be easily drawn from the spatial arc L are recommended to compute the knotting probabilities of L. By Corollary 3.1, the 12 arc diagrams D(±L;±x), D(±L;±y) and D(±L;±z) of the spatial arc L are proposed. In this section, the knotting probabilities of three concrete examples of even arc knots are computed as Examples A, B and C.

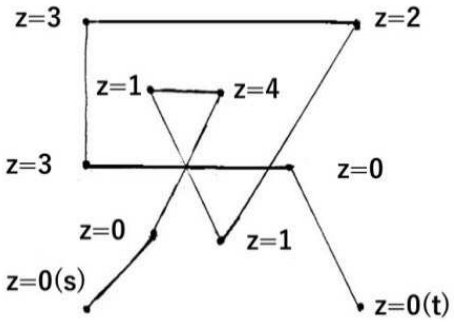

Figure 2. *The spatial arc L given by the vertex coordinate data: namely, the (x, y) vertex coordinates (0, 0), (1, 1), (2, 3), (1, 3), (2, 1), (4, 4), (0, 4), (0, 2), (3, 2), (4, 0) of λ_z (L) in the xy plane and the z vertex coordinate data in the figure.*

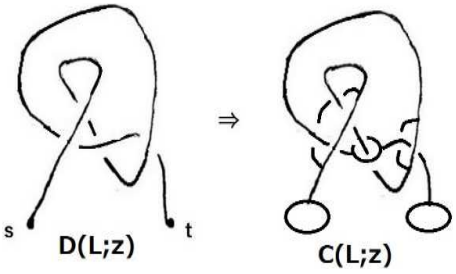

Figure 3. *Producing the chord diagram C(L;z) and a simplified chord diagram from the projection image $\lambda_z(L)$.*

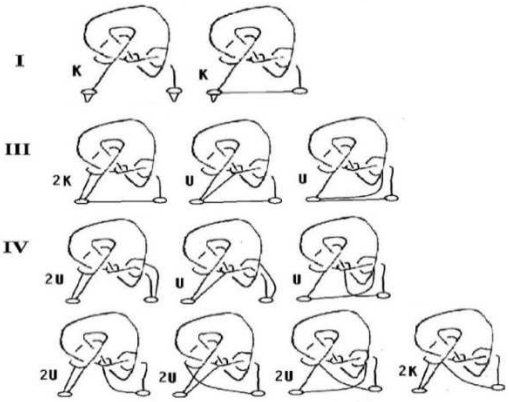

Figure 4. *Calculations on the chord diagram C(L;z).*

Example A. Consider an even arc knot L in Figure 2 given by the projection image $\lambda_z(L)$ in the xy plane together with the z-coordinate such that the vertex coordinates $(x, y, z)=(x, y)^z$ of L ordered from the starting point s are given by $(0, 0)^0$, $(1, 1)^0$, $(2, 3)^4$, $(1, 3)^1$, $(2, 1)^1$, $(4, 4)^2$, $(0, 4)^3$, $(0, 2)^3$, $(3, 2)^0$, $(4, 0)^0$. The closed knot cl(L) is a trefoil knot. The arc diagram D(L;z) obtained from $\lambda_z(L)$ is illustrated in the left side of Figure 3. In computing the knotting probability p(L;z) from the chord diagram C(L;z) of the arc diagram D(L;z), a simplified chord diagram of the chord diagram C(L;z) given by the following observation is used to make the computation simpler.

Observation 4.1. If two based loops are connected by a chord not intersecting the other chords, one can replace the two based loops with the chord by one based loop without changing the knotting probability.

In the right side of Figure 3, a simplified chord diagram of the chord diagram C(L;z) is given. In the use of a simplified chord diagram obtained by using Observation 4.1, a carefulness is needed in counting the knotted and unknotted adjoint chord diagrams. In fact, a calculation on the numbers of the knotted and unknotted adjoint chord diagrams of the chord diagram C(L;z) is done by using a simplified chord diagram of C(L;z) as in Figure 4 (see the paper [10] for the details of the calculation). The following calculation results are obtained:

$$p(L;\pm z) = p(-L;\pm z) = (1, \tfrac{1}{2}, \tfrac{1}{2}, \tfrac{1}{6})$$

by Corollary 3.1, for L is an even spatial arc and D(L;z) is an inbound arc diagram.

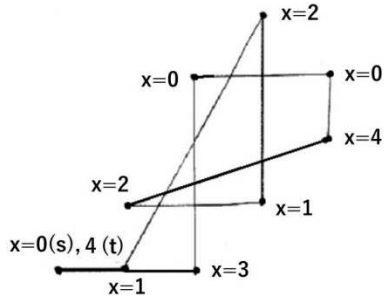

Figure 5. *The spatial arc L given by the vertex coordinate data: namely, the (y, z) vertex coordinates (0, 0), (1, 0), (3, 4), (3, 1), (1, 1), (4, 2), (4, 3), (2, 3), (2, 0), (0, 0) of $\lambda_x(L)$ in the yz plane and the x vertex coordinate data in the figure.*

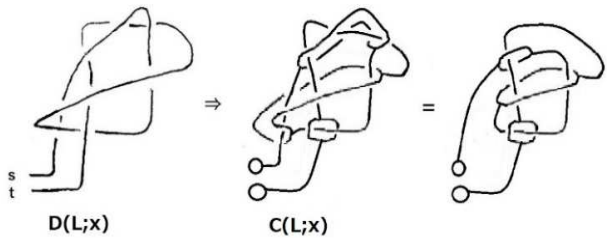

Figure 6. *Producing the chord diagram C(L;x) and a simplified chord diagram from the projection image $\lambda_x(L)$.*

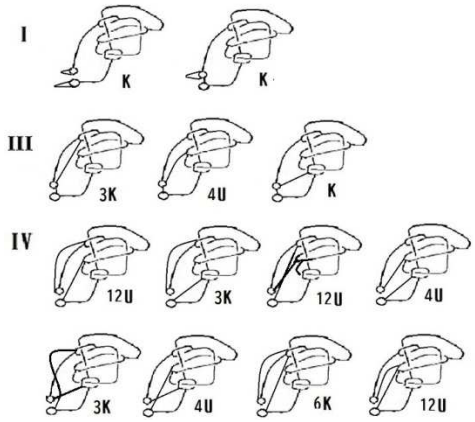

Figure 7. *Calculations on the chord diagram C(L;x).*

In Figure 5, the same arc knot L is presented by the projection image $\lambda_x(L)$ in the yz plane together with the x-coordinate such that the vertex coordinates (x, y, z) = $(y, z)^x$ of L ordered from the starting point s are given by$(0, 0)^0$, $(1, 0)^1$, $(3, 4)^2$, $(3, 1)^1$, $(1, 1)^2$, $(4, 2)^4$, $(4, 3)^0$, $(2, 3)^0$, $(2, 0)^3$, $(0, 0)^4$. The arc diagram D(L;x) obtained from $\lambda_x(L)$ is illustrated in Figure 6, where the chord diagram C(L;x) and a simplified chord diagram are also illustrated. A calculation on the numbers of the knotted and unknotted adjoint chord diagrams of the chord diagram C(L;x) using the simplified chord diagram of C(L;x) is done in Figure 7. Then the following calculation results are obtained:

$$p(L;\pm x)=p(-L;\pm x) =(1,\frac{1}{2},\frac{1}{2},\frac{3}{14})$$

by Corollary 3.1, for L is an even arc knot and D(L;x) is an inbound arc diagram.

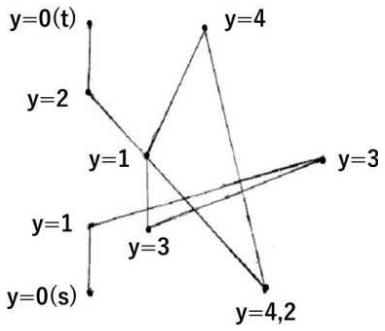

Figure 8. *The spatial arc L given by the vertex coordinate data: namely, the (z, x) vertex coordinates (0, 0), (0, 1), (4, 2), (1, 1), (1, 2), (2, 4), (3, 0), (3, 0), (0, 3), (0, 4) of $\lambda_y(L)$ in the zx plane and the y vertex coordinate data in the figure.*

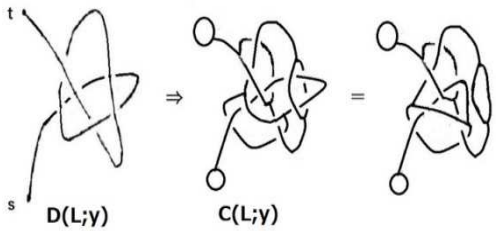

Figure 9. *Producing the chord diagram C(L;y) and a simplified chord diagram from the projection image $\lambda_y(L)$.*

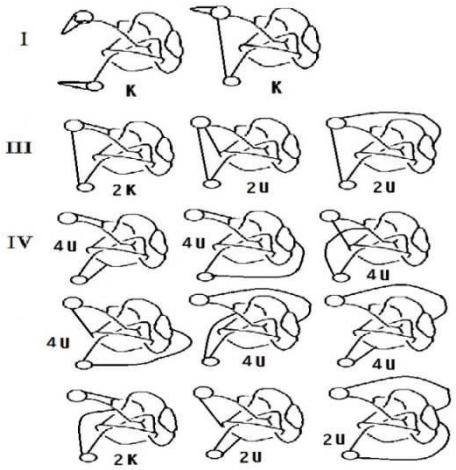

Figure 10. *Calculations on the chord diagram C(L;y).*

In Figure 8, the same arc knot L is presented by the projection image $\lambda_y(L)$ in the zx plane together with the y-coordinate such that the vertex coordinates (x, y, z) = $(z, x)^y$ of L ordered from the starting point s are given by $(0, 0)^0$, $(0, 1)^1$, $(4, 2)^3$, $(1, 1)^3$, $(1, 2)^1$, $(2, 4)^4$, $(3, 0)^4$, $(3, 0)^2$, $(0, 3)^2$, $(0, 4)^0$. The arc diagram D(L;y) obtained from $\lambda_y(L)$ is illustrated in Figure 9, where the chord diagram C(L;y) and a simplified chord diagram are also illustrated. A calculation on the numbers of the knotted and unknotted adjoint chord diagrams of the chord diagram C(L;y) using the simplified chord diagram of C(L;y) is done in Figure 10. Then the following calculation results are obtained:

$$p(L;\pm y)=p(-L;\pm y) =(1,\frac{1}{2},\frac{1}{2},\frac{1}{5})$$

by Corollary 3.1, for L is an even arc knot and D(L;y) is an inbound arc diagram.

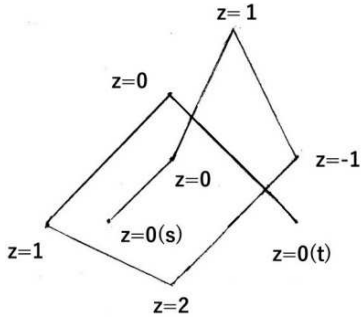

Figure 11. *The spatial arc L given by the vertex coordinate data: namely, the (x, y) vertex coordinates (0, 0), (1, 1), (2, 3), (3, 1), (1,-1), (-1, 0), (1, 2), (3, 0) of $\lambda_z(L)$ in the xy plane and the z vertex coordinate data in the figure.*

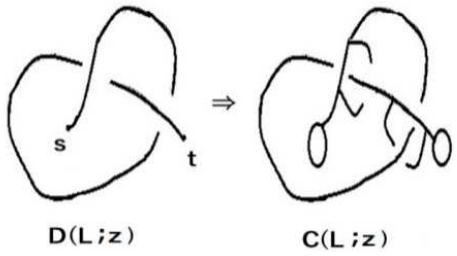

Figure 12. *Producing the arc diagram D(L;z) and the chord diagram C(L;z).*

Example B. Consider an even arc knot L in Figure 11 given by the non-inbound projection image $\lambda_z(L)$ in the xy plane together with the z-coordinate such that the vertex coordinates (x, y, z) = $(x, y)^z$ of L ordered from the starting point s are given by $(0, 0)^0$, $(1, 1)^0$, $(2, 3)^1$, $(3, 1)^{-1}$, $(1,-1)^2$, $(-1, 0)^1$, $(1, 2)^0$, $(3, 0)^0$. The closed knot cl(L) is also a trefoil knot. The arc diagram D(L;z) and the chord diagram C(L;z) obtained from λ_z (L) are illustrated in Figure 12. The knotting probability of the chord diagrams C(L;±z) of the arc diagrams D(L;±z) has been computed in [10]. The following calculation results are obtained:

$$p(L;\pm z) = (\tfrac{1}{2}, \tfrac{1}{2}, 0, \tfrac{1}{2}),\ p(-L;\pm z) = 0.$$

In Figure 13, the same arc knot L is presented by the projection image $\lambda_x(L)$ in the yz plane together with x-coordinate information such that the vertex coordinates (x, y, z) = $(y, z)^x$ of L ordered from the starting point s are given by$(0, 0)^0$, $(1, 0)^1$, $(3, 1)^2$, $(1,-1)^3$, $(-1, 2)^1$, $(0, 1)^{-1}$, $(2, 0)^1$, $(0, 0)^3$. The arc diagram D(L;x) obtained from $\lambda_x(L)$ is illustrated in Figure 14, where the chord diagram C(L;x) and a simplified chord diagram are also illustrated. A calculation on the numbers of the knotted and unknotted adjoint chord diagrams of the chord diagram C(L;x) using the simplified chord diagram of C(L;x) is done in Figure 15. Then the following calculation results are obtained:

$$p(L;\pm x)=p(-L;\pm x) =(1, \tfrac{1}{3}, \tfrac{1}{3}, \tfrac{1}{15})$$

by Corollary 3.1, for L is an even arc knot and D(L;x) is an inbound chord diagram.

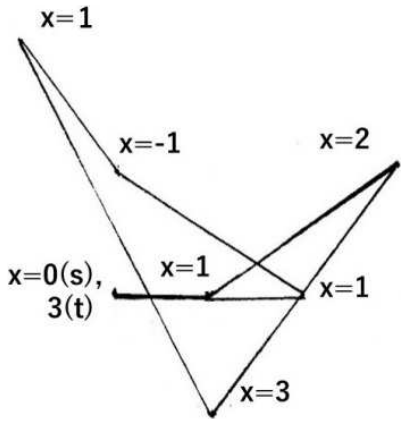

Figure 13. *The spatial arc L given by the vertex coordinate data: namely, the (y, z) vertex coordinates (0, 0), (1, 0), (3, 1), (1,-1), (-1, 2), (0, 1), (2, 0), (0, 0) of $\lambda_x(L)$ in the yz plane and the x vertex coordinate data in the figure.*

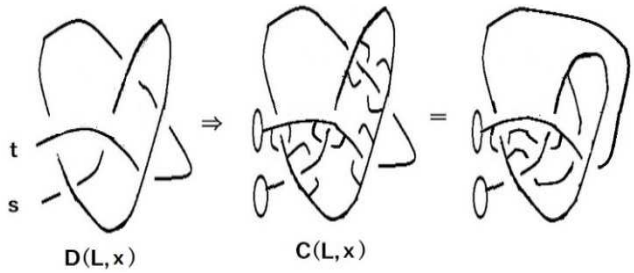

Figure 14. *Producing the chord diagram C(L;x) and a simplified chord diagram from the projection image $\lambda_x(L)$.*

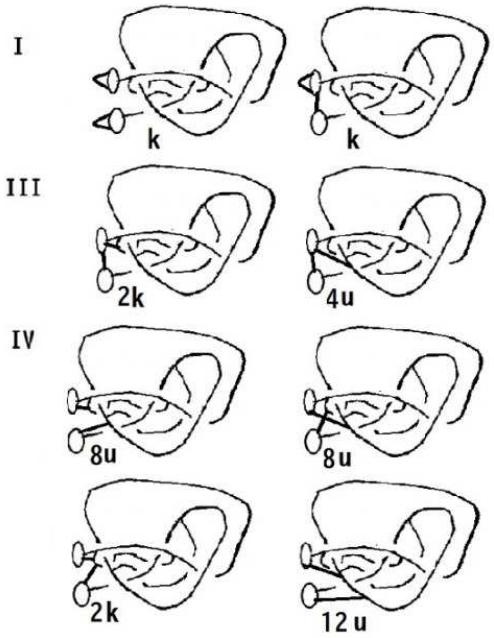

Figure 15. *Calculations on the chord diagram C(L;x).*

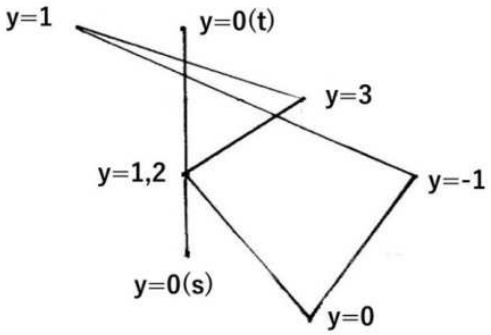

Figure 16. *The spatial arc L given by the vertex coordinate data: namely, the (z, x) vertex coordinates (0, 0), (0, 1), (1, 2), (-1, 3), (2, 1), (1,-1), (0, 1), (0, 3) of $\lambda y(L)$ in the zx plane and the y vertex coordinate data in the figure.*

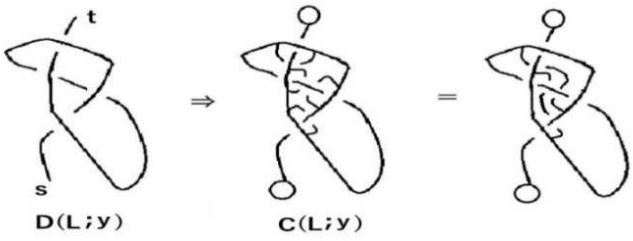

Figure 17. *Producing the arc diagram D(L;y), the chord diagram C(L;y) and a simplified chord diagram from the projection image $\lambda_y(L)$.*

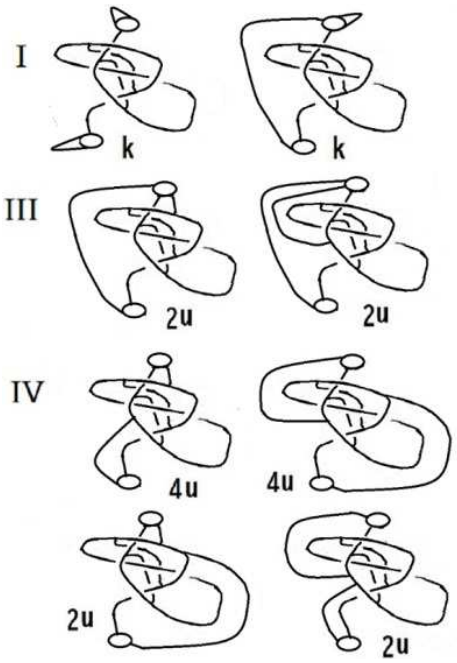

Figure 18. *Calculations on the chord diagram C(L;y).*

In Figure 16, the same arc knot L is presented by the projection image $\lambda_y(L)$ in the zx plane together with y-coordinate information such that the vertex coordinates (x, y, z) = (z, x)^y of L ordered from the starting point s are given by $(0, 0)^0$, $(0, 1)^1$, $(1, 2)^3$, $(-1, 3)^1$, $(2, 1)^{-1}$, $(1,-1)^0$, $(0, 1)^2$, $(0, 3)^0$. The arc diagram D(L;y) obtained from $\lambda_y(L)$ is illustrated in Figure 17, where the chord diagram C(L;y) and a simplified chord diagram are also illustrated. A calculation on the numbers of the knotted and unknotted adjoint chord diagrams of the chord diagram C(L;y) using the simplified chord diagram of C(L;y) is done in Figure 18. Then the following calculation results are obtained:

$$p(L;\pm y) = p(-L;\pm y) = (1,0, 0, 0)$$

by Corollary 3.1, for L is an even arc knot and D(L;y) is an inbound chord diagram.

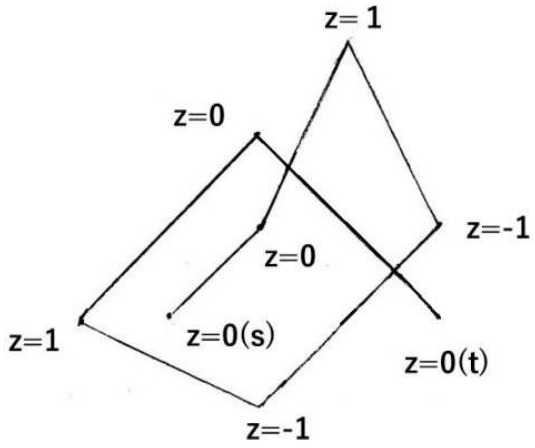

Figure 19. *The spatial arc L given by the vertex coordinate data: namely, the (x, y) vertex coordinates (0, 0), (1, 1), (2, 3), (3, 1), (1,-1), (-1, 0), (1, 2), (3, 0) of $\lambda_z(L)$ in the xy plane and the z vertex coordinate data in the figure.*

Example C. Consider an even arc knot L in Figure 19 given by the non-inbound projection image $\lambda_z(L)$ in the xy plane together with the z-coordinate such that the vertex coordinates (x, y, z) = (x, y)^z of L ordered from the starting point s are given by$(0, 0)^0$, $(1, 1)^0$, $(2, 3)^1$, $(3, 1)^{-1}$, $(1,-1)^{-1}$, $(-1, 0)^1$, $(1, 2)^0$, $(3, 0)^0$. Note that the closed knot cl(L) is a trivial knot. The arc diagram D(L;z) coincides with the arc diagram D(L;z) in Example B. Thus, the following calculation results are obtained:

$$p(L;\pm z)=(\tfrac{1}{2},\tfrac{1}{2},0,\tfrac{1}{2}),\ p(-L;\pm z) =0.$$

This means that even if the closed knot cl(L) of an even arc knot L is a trivial knot, the knotting probability p(L;u) may not be zero for a general unit vector u.

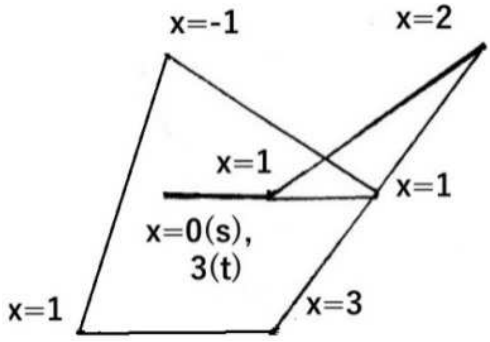

Figure 20. *The spatial arc L given by the vertex coordinate data: namely, the (y, z) vertex coordinates (0, 0), (1, 0), (3, 1), (1,-1), (-1, 2), (0, 1), (2, 0), (0, 0) of $\lambda_x(L)$ in the yz plane and the x vertex coordinate data in the figure.*

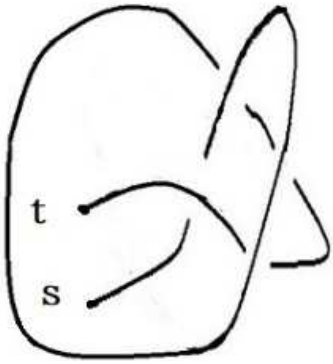

Figure 21. *Producing the arc diagram D(L;x).*

In Figure 20, the same arc knot L is presented by the projection image $\lambda_x(L)$ in the yz plane together with the x-coordinate such that the vertex coordinates (x, y, z) = (y, z)^x of L ordered from the starting point s are given by $(0, 0)^0$, $(1, 0)^1$, $(3, 1)^2$, $(1,-1)^3$, $(-1,-1)^1$, $(0, 1)^{-1}$, $(2, 0)^1$, $(0, 0)^3$. The arc diagram D(L;x) obtained from $\lambda_x(L)$ is illustrated in Figure 21 and is an inbound arc diagram whose under-closed knot diagram $cl_u(D(L;x))$ (that is, a knot diagram obtained from D(L;x) by joining the endpoints with an under-arc) represents a trivial knot. This means the following calculation results (see the paper [10;Theorem 3.3 (1)] for the proof):

$$p(L;\pm x)=p(-L;\pm x) =0.$$

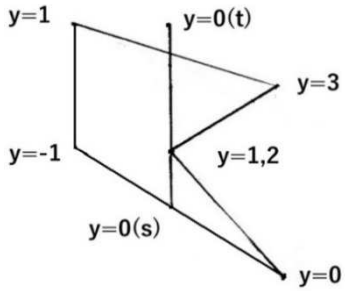

Figure 22. *The spatial arc L given by the vertex coordinate data: namely, the (z, x) vertex coordinates (0, 0), (0, 1), (1, 2), (-1, 3), (2, 1), (1,-1), (0, 1), (0, 3) of $\lambda_y(L)$ in the zx plane and the y vertex coordinate data in the figure.*

Figure 23. *Producing the arc diagram D(L;y).*

In Figure 22, the same arc knot L is presented by the projection image $\lambda_y(L)$ in the zx plane together with the y-coordinate such that the vertex coordinates $(x, y, z) = (z, x)^y$ of L ordered from the starting point s are given by$(0, 0)^0$, $(0, 1)^1$, $(1, 2)^3$, $(-1, 3)^1$, $(-1, 1)^{-1}$, $(1,-1)^0$, $(0, 1)^2$, $(0, 3)^0$. The arc diagram D(L;y) obtained from $\lambda_y(L)$ is illustrated in Figure 23 and isomorphic to the inbound arc diagram given in the paper [10; Example 4.5], where the knotting probability is calculated. Then the following calculation results are obtained:

$$p(L;\pm y)=p(-L;\pm y) =(1, \tfrac{1}{3}, \tfrac{1}{3}, 0).$$

5. Conclusion

Given the data of a spatial arc, a procedure to construct characteristic arc diagrams and their chord diagrams and adjoint chord diagrams is shown in this paper. It is hoped that a computer use will, hopefully, configure the procedure up to this point fairly automatically.

Acknowledgements

This work was partly supported by JSPS KAKENHI Grant Numbers JP19H01788, JP21H00978 and Osaka Central Advanced Mathematical Institute, Osaka Metropolitan University (MEXT Joint Usage/Research Center on Mathematics and Theoretical Physics JPMXP 0619217849).

References

[1] R. H. Crowell and R. H. Fox, Introduction to knot theory (1963) Ginn and Co.; Re-issue Grad. Texts Math., 57 (1977), Springer Verlag.

[2] T. Deguchi and T. Tsurusaki, A statistical study of random knotting using the Vassiliev invariants, J. Knot Theory Ramifications, 3 (1994), 321-353.

[3] A. Kawauchi, A survey of knot theory, Birkhäuser (1996).

[4] A. Kawauchi, On transforming a spatial graph into a plane graph, Statistical Physics and Topology of Polymers with Ramifications to Structure and Function of DNA and Proteins, Progress of Theoretical Physics Supplement, 191 (2011), 235-244.

[5] A. Kawauchi, A chord diagram of a ribbon surface-link, J. Knot Theory Ramifications, 24 (2015), 1540002 (24pp.).

[6] A. Kawauchi, Knot theory for spatial graphs attached to a surface, Contemporary Mathematics, 670 (2016), 141-169.

[7] A. Kawauchi, Supplement to a chord diagram of a ribbon surface-link, J. Knot Theory Ramifications, 26 (2017) 1750033 (5pp.).

[8] A. Kawauchi, A chord graph constructed from a ribbon surface-link, Contemporary Mathematics, 689 (2017), 125-136. Amer. Math. Soc., Providence, RI, USA.

[9] A. Kawauchi, Faithful equivalence of equivalent ribbon surface-links, J. Knot Theory Ramifications, 27, No. 11 (2018), 1843003 (23 pages).

[10] A. Kawauchi, Knotting probability of an arc diagram, Journal of Knot Theory Ramifications 29 (10) (2020) 2042004 (22 pages).

[11] A. Kawauchi, T. Shibuya and S. Suzuki, Descriptions on surfaces in four-space, I: Normal forms, Math. Sem. Notes, Kobe Univ., 10 (1982), 75-125; II: Singularities and cross-sectional links, Math. Sem. Notes, Kobe Univ. 11 (1983), 31-69.

[12] K. Millett, A. Dobay and A. Stasiak, Linear random knots and their scaling behavior, Macromolecules, 38, (2005) 601-606.

[13] E. Uehara and T. Deguchi, Knotting probability of self-avoiding polygons under a topological constraint, J. Chemical Physics, 147, 094901 (2017).

[14] V. Veblen and J. W. Young, Projective geometry, Ginn and Company, (1910), Boston, Massachusetts, U.S.A.

[15] T. Yanagawa, On ribbon 2-knots I; the 3-manifold bounded by the 2-knot, Osaka J. Math., 6 (1969), 447-464.